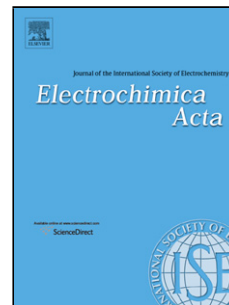


Accepted Manuscript

Title: Magnetically controlled electrochemical sensing membrane based on multifunctional molecularly imprinted polymers for detection of insulin

Author: Wanying Zhu Lei Xu Chunhong Zhu Bingzhi Li
Hong Xiao Huijun Jiang Xuemin Zhou



PII: S0013-4686(16)32026-6
DOI: <http://dx.doi.org/doi:10.1016/j.electacta.2016.09.108>
Reference: EA 28038

To appear in: *Electrochimica Acta*

Received date: 13-4-2016
Revised date: 14-9-2016
Accepted date: 21-9-2016

Please cite this article as: Wanying Zhu, Lei Xu, Chunhong Zhu, Bingzhi Li, Hong Xiao, Huijun Jiang, Xuemin Zhou, Magnetically controlled electrochemical sensing membrane based on multifunctional molecularly imprinted polymers for detection of insulin, *Electrochimica Acta* <http://dx.doi.org/10.1016/j.electacta.2016.09.108>

This is a PDF file of an unedited manuscript that has been accepted for publication. As a service to our customers we are providing this early version of the manuscript. The manuscript will undergo copyediting, typesetting, and review of the resulting proof before it is published in its final form. Please note that during the production process errors may be discovered which could affect the content, and all legal disclaimers that apply to the journal pertain.

**Magnetically Controlled Electrochemical Sensing
Membrane based on Multifunctional Molecularly Imprinted
Polymers for Detection of Insulin**

Wanying Zhu^a, Lei Xu^a, Chunhong Zhu^a, Bingzhi Li^a, Hong Xiao^b, Huijun Jiang^a,
Xuemin Zhou^{a,*}

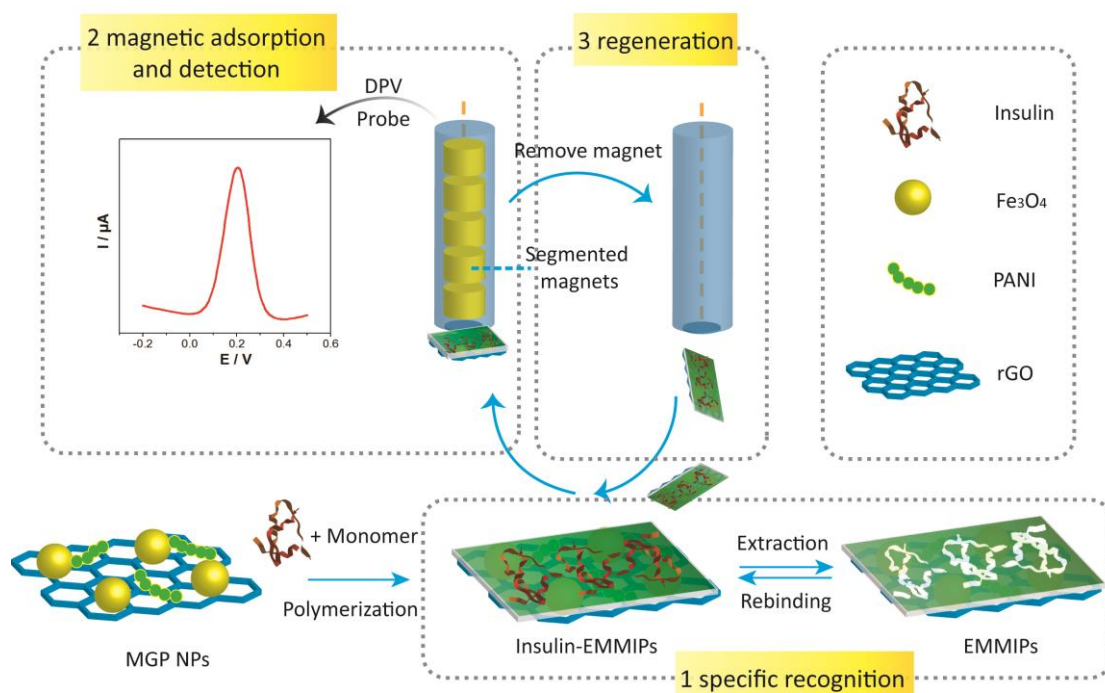
^aSchool of Pharmacy, Nanjing Medical University, Nanjing 211166, PR China

*^bDepartment of Neuro-Psychiatric Institute, Nanjing Brain Hospital Affiliated to
Nanjing Medical University, Nanjing 210029, PR China*

*Corresponding Author. Tel.: +86 25 86868476. Fax: +86 25 86868476.

E-mail: xueminzhou001_001@hotmail.com. (X. M. Zhou)

Graphical abstract



Highlights:

1. As supporting materials for EMMIPs-based sensor, the ternary MGP NPs show great conductivity and electrocatalytical activity.
2. The multifunctional EMMIPs with large surface area, excellent conductivity, magnetic response and selectivity recognition properties were obtained on the surface of ternary MGP NPs under mild condition.
3. A facile and controllable EMMIPs-based sensor was fabricated by magnetic field directed self-assembly and the factors affecting the fabrication of the sensor were studied.
4. All steps of this method were completed independently, so the efficiency of the analysis was improved, promoting its application in high throughput analysis of biomacromolecular for clinical diagnosis.

Abstract

A magnetically controlled electrochemical sensing membrane for detection of insulin was fabricated by magnetic field directed self-assembly of electromagnetic molecularly imprinted polymers (EMMIPs). EMMIPs with excellent electrochemical performance and multiple recognition sites to insulin were synthesized by surface polymerization on the ternary $\text{Fe}_3\text{O}_4@\text{rGO}/\text{PANI}$ nanoparticles (MGP NPs). The insulin-EMMIPs obtained by recognizing insulin from sample were assembled onto a magnetic glassy carbon electrode (MGCE) surface in order to form the magnetically controlled membrane under the magnetic field induction, and the membrane was peeled off from the electrode by removal of the magnet after electrochemical measurement. In this work, the biomimetic sensing membrane could be controlled more effectively and the electrode could be regenerated more conveniently. The novel magnetically controlled sensing membrane showed good selectivity and reproducibility for the determination of insulin with the detection limit reaching 17 pM ($S/N=3$), and this limit of detection was further reduced to 3 pM by using the $\text{Fe}(\text{CN})_6^{3-/4-}$ redox probe. It has potential applications in the fields of clinical diagnosis with real-time detection capability, high efficiency, and easy operation properties.

Keywords: Electrochemical sensing membrane; $\text{Fe}_3\text{O}_4@\text{rGO}/\text{PANI}$ nanoparticles (MGP NPs); Electromagnetic molecularly imprinted polymers (EMMIPs); Magnetic field directed self-assembly; Insulin

1. Introduction

Diabetes is a metabolic disorder in which aberrant glucose metabolism appears owing to insulin deficiency (type 1 or juvenile diabetes) or to loss of insulin action (type 2 or insulin-resistant diabetes). [1-2] Insulin is a polypeptide hormone produced in the pancreas, which is vital for controlling glucose metabolism.[3] The determination of insulin is of significant value in the clinical classification of types of diabetes and the diagnosis of related diseases (e.g. insulinoma and trauma). However, the low level of insulin in blood serum (on the order of picomolar) warrants the development of highly sensitive assay methods.

Numerous detection methods for insulin have been reported, such as radioimmunoassay,[4] fluorescence resonance energy transfer (FRET),[5] enzyme-linked immunosorbent assay (ELISA),[6] MALDI-TOF mass spectrometry,[7] electrochemical method.[1, 8-10] Some of these strategies share several bottlenecks including the involvement of time-consuming operation steps, requirement of complex instruments and well-trained operators, consumption of expensive antibodies and radioisotopes, etc.[1-2] Among them, electrochemical method has attracted tremendous attention because of its high sensitivity, low cost, rapid response and more importantly, the possibility to construct portable devices easy to use for point of care.[1, 8-10]

As a key component in the sensor system, the sensing agent has been explored intensively both in material itself and in modification strategy. Among multifarious approaches, the molecular imprinting technique, which possesses specific binding

sites complementary in size and shape to templates, has become a useful tool for the fabrication of sensitive agents with a predetermined recognition ability for the template molecules.[11-14] To date, although creating molecularly imprinted polymers (MIPs) for small molecule have been well established, whereas the success of imprinting of macromolecules (like proteins) is still a challenge. Major difficulties are summarized as follows: (i) the insolubility of proteins in commonly utilized imprinting solvents, (ii) the degradation of proteins under polymerization conditions such as high temperature, (iii) the large molecular size and structural complexity which restrict their diffusivity.[15-17] Surface imprinting is quite attractive for imprinting protein as the imprinted sites are close to or at the surface of MIPs avoiding the protein embedment in the polymer matrix, and thereby making the elution and rebinding of the target protein easy.[18-20] As an alternative, MIPs with multiple binding sites were explored invoking surface molecular imprinting in an aqueous media with mild preparation conditions.

Up to now, various materials, such as magnetic nanoparticles,[21-22] nanowires/nanotubes,[23-24] quantum dots,[25] polymer NPs,[26] and silica NPs[27] were chosen to be solid supporting materials for surface molecular imprinting protein. However, these works mainly focused on the investigation of protein rebinding and recognition properties. Thus, exploration of new nanomaterials in fabricating MIPs-based sensors is quite necessary to improve the electro-catalytic activity, the recognition feature and the adsorption performance for the target molecules.[28-30] In our previous study,[11] we found that it could be a satisfactory alternative for

preparing the ternary electromagnetic nanoparticles by the combination of Fe_3O_4 , polyaniline (PANI) and the reduced graphene oxide (rGO) due to the special magnetism of Fe_3O_4 and the excellent electrical conductivity of both PANI and rGO. The ternary electromagnetic Fe_3O_4 @PANI/rGO nanoparticles were successfully served as the monomer in the fabrication of molecularly imprinted polymer membrane by electro-polymerization, providing a promoting pathway for electron transfer. In present study, considering the stability and binding sites of nanoparticles, the synthesis method has been improved. The novel ternary Fe_3O_4 @rGO/PANI nanoparticles (MGP NPs) were obtained by the in situ formation of Fe_3O_4 nanoparticles into the graphene oxide layers followed by hydrazine hydrate reduction, and further oxidative polymerization of aniline to generate the composite. The MGP NPs could not only provide multiple functionalized binding sites in the matrix to form hydrogen bond, hydrophobic action and π - π stacking interaction with insulin, but also afford a promoting network for electron transfer. However, to our best knowledge, no reports have focused on the imprinting protein on the surface of the ternary electromagnetic nanoparticles by in situ polymerization.

So far there are many novel strategies for constructing MIP-based electrochemical sensor. Among them, electro-polymerization was one of the most widely used approaches.[11-12, 31-33] However, a traditional MIP-based electrochemical sensor fabricated by electro-polymerization possesses tedious electrode modifications and the process of electrode regeneration is difficult. For this reason, the fabrication of a common sensor suitable for batching measuring was of

great significance in the clinical diagnosis. Directed self-assembly of nanocomposites is one of the most promising approaches for preparing novel materials and devices with desired morphologies and properties.[34] There are two broad divisions containing template-guided self-assemblies (e.g. physical template, chemical template and biological template) and field-guided self-assemblies (e.g. magnetic field, electric field, pressure gradient, light and laser).[35-36] In our previous studies, magnetic field directed self-assembly has been confirmed as an efficient, convenient and timesaving approach to construct the orderly and oriented geometric nanostructure.[11, 37-38] Magnetic field directed self-assembly by magnetic glassy carbon electrode (MGCE) allows a controllable rebinding process and permits easy and quick magnetic separation. Therefore, the use of MGCE and EMMIPs allows electrochemical detection and eliminates the problem of regeneration difficulty that occurs with traditional electrode systems.

Herein, a facile and controllable EMMIPs-based electrochemical sensor for the detection of insulin was fabricated by magnetic field directed self-assembly of EMMIPs by MGCE. The EMMIPs obtained on the surface of the ternary MGP NPs under mild conditions show high selectivity to recognize the template protein from the complex samples as well as good electrochemical properties. By installing or removing the magnet of the electrode, the immobilization and removal of EMMIPs on the electrode surface could be controlled flexibly. Meanwhile, the regeneration of the modified electrodes was greatly speeded up. For this strategy, the elution and recognition of the template molecule insulin could be completed independently

without electrode, promoting its application in the analysis of clinical samples with high throughput. The ternary MGP NPs were characterized by CV, FT-IR, Raman, XPS and TEM to investigate electrochemical performance, composition and morphology, respectively. The sensors fabricated with different magnetic field strength were analyzed by AFM to compare their microstructures, suggesting that the morphologies of the membrane could be easily controlled by magnetic field directed self-assembly. Furthermore, the EMMIPs-based electrochemical sensor was employed to detect insulin in biological samples.

2. Experimental

2.1 Reagents and materials

Horseradish peroxidase (HRP) and dopamine (DA) were purchased from Aladdin Reagent Co., Ltd. (Shanghai, China). Ascorbic acid (AA), Bovine hemoglobin (BHB), and uric acid (UA) were obtained from Sinopharm Chemical Reagent Co., Ltd. (Shanghai, China). Glutathione (GSH) was purchased from Xiya reagent Co., Ltd. (Sichuan, China). Human insulin and bovine serum albumin (BSA) were purchased from Sigma Aldrich (St. Louis, USA). Ammonium persulfate and aniline were purchased from Shanghai Lingfeng Chemical Reagent Co., Ltd. (Shanghai, China). The commercial insulin radioimmunoassay kit was purchased from Beijing North Institute of Biotechnology (Beijing, China). The phosphate buffer solution (PBS) was prepared by mixing the stock solution of NaH_2PO_4 and Na_2HPO_4 while the Tris-HCl buffer was prepared by mixing the stock solution of Tris and HCl.

2.2 Apparatus

The electrochemical measurements were performed in a conventional three-electrode cell, using a CHI 660D workstation (Shanghai Chenhua Co., China) with a platinum electrode as the counter electrode and a saturated calomel electrode (SCE) as the reference electrode. The magnetic glassy carbon electrode (MGCE, $\Phi=5$ mm, magnetic field strength = 0.032 T/segment, totally 10 segments, shown in Fig. S1) was purchased from Tianjin Incole Union Technology Co., Ltd. (Tianjin, China). Scanning electron microscope (SEM) images were recorded with S-4800 (Hitachi, Japan). Atomic force microscope (AFM) images were obtained by Dimension Icon (Bruker, USA). X-ray photoelectron spectroscopy (XPS) measurements were performed using a PHI Quantera II spectrometer (Japan) and samples were freeze-dried before assay. Transmission electron microscope (TEM) images were collected using JEM2010F (JEOL, Japan). The results by radioimmunoassay were measured by a GC-911 γ counter.

2.3 Synthesis of MGP NPs

Graphene oxide (GO) was firstly synthesized by a modified Hummers method and then Fe_3O_4 @rGO composites were synthesized according to our previous reports with a little modification.[37] Briefly, 230 mg GO was dispersed in 80 mL deionized water by ultrasonic for 1 h. Then, 1.72 g $\text{FeCl}_2\cdot 4\text{H}_2\text{O}$ and 4.72 g $\text{FeCl}_3\cdot 6\text{H}_2\text{O}$ in 30 mL water were added to GO solution under nitrogen flow with vigorous stirring for 1 h. After that, 10 mL aqueous ammonia was added dropwise for synthesis of Fe_3O_4 nanoparticles. The temperature of the solution rose to 80 °C and 1.6 mL hydrazine hydrate was added for the reduction of GO. After rapid stirring for 10 h, the obtained

black Fe₃O₄@rGO composites were collected by external magnetic field, washed by ethanol, deionized water successively, then dried in vacuum.

Fe₃O₄@PANI/rGO composites (MGP NPs) were prepared as follows: To a stirred solution of 0.83 g Fe₃O₄@rGO in 100 mL deionized water (containing 0.25 mM HCl), 5 mL of 1.75 M aniline was added for another 30 min stir. Subsequently, 5 mL of 0.35 M ammonium persulfate was added dropwise. After continuous rapidly stirring for 4 h at 0-5 °C, the obtained black MGP NPs were separated by external magnetic field, washed with deionized water until neutral and then stored in 50 mL nitrogen saturated deionized water at 4 °C.

2.4 Preparation of EMMIPs

The monomer (MGP NPs, 100 mg/20 mL 0.2 M pH 7.4 Tris-HCl buffer), template (insulin, 16 mg/10 mL 0.01 M HCl) and the both co-monomer and cross-linker (aniline, 0.03 M, 5 mL) were mixed together and stirred moderately for 2 h under nitrogen protection to complete the pre-assembly through hydrogen bonding, π - π stacking and hydrophobic interactions. Then, 5 mL of 6 mM ammonium persulfate solution was added and the mixture was stirred continually at 0-4 °C for another 4 h to complete the reaction. Subsequently, in the elution procedure, 20 mL of 2 M HAc:MeCN (1:4) was mixed with the separated nanocomposites, and treated for 40 min to remove the template insulin. Electromagnetic non-imprinted polymers (EMNIPs) were prepared following the above steps without template for comparison. The route for the preparation of EMMIPs was shown in Scheme 1.

2.5 Fabrication of EMMIPs-based sensor

For insulin determination, 10 mg of EMMIPs were dispersed in 4 mL of Tris-HCl buffer solution (0.1 M, pH 7.4) containing different concentrations of insulin, and then were shaken continuously using a vortex mixer for 20 min. Insulin-EMMIPs were obtained by selectively adsorption and recognition of insulin, and 0.5 mL of them were separated from the solution and then transferred into 1.5 mL 0.1 M KCl-PB solution (0.02 M, pH 7.4). Next, a MGCE with the magnet was inserted into the solution slowly and maintained in a vertical position, leading to accumulation of EMMIPs on the MGCE surface. The EMMIPs-based sensor was obtained after 5 min, and then the DPV electrochemical signal was measured. After use, the electrode was regenerated by removal of the magnet within the electrode. The process for the fabrication of the EMMIPs-based sensor and the detection process were shown in Scheme 1. In order to reveal the specialty of the as-prepared sensor, a traditional molecularly imprinted electrochemical sensor (MIES) was fabricated by electro-polymerization following the similar procedure described above and the electro-polymerization was conducted according to our previous study.[38]

Scheme 1 here

2.6 Serum Sample Analysis

Human serum samples were obtained from the People's Hospital of Gaochun. They were firstly treated with filtration using Amicon® Ultra 10K centrifugal filter (Millipore Corp., USA), and then 500 μ L filtrate was diluted with equal amount of Tris-HCl buffer solution (0.2 M, pH 7.4). The analysis process was conducted similarly to the fabrication of EMMIPs-based sensor detailed in section 2.5. For

comparison study, they were also measured by radioimmunoassay clinically used.

3. Results and discussion

3.1 Characterization of the ternary MGP NPs

The elemental components of ternary MGP NPs are analyzed by XPS (Fig. 1A), indicating the co-existence of C, N, O, and Fe elements in the ternary MGP NPs. The Fe 2p XPS spectra of the nanocomposite (inset in Fig. 1A) exhibit binding energy peaks at 710.6 eV (Fe 2p_{3/2}) and 723.9 eV (Fe 2p_{1/2}), suggesting the existence of Fe₃O₄. [39] The C 1s spectra (Fig. 1B) can be deconvoluted into five peaks, the peaks at binding energies of 284.6, 285.5, 286.5, 288.3, and 289.1 eV are ascribed to the C=C, C-N, C-O, C=O, and O-C=O species, respectively. [40] Compared to C 1s spectra of GO [40], an additional peak at around 285.5 eV (C-N) suggested the presence of PANI in the ternary MGP NPs. Besides, due to the reduction of graphene oxide by hydrazine hydrate, the peak intensities of the oxygenated carbon become much weaker. As shown in Fig. 1C, the N 1s spectra can be resolved into three individual component peaks centered at 398.2, 400.0 and 401.2 eV, corresponding to the quinoid imine (=N-), the benzenoid amine (-NH-) and the cationic nitrogen atoms (-N⁺-), respectively. [39, 41] All these peaks are characteristic to the doped PANI.

Moreover, the FT-IR spectra and Raman spectra are used to characterize the structure and composition of GO, Fe₃O₄@rGO and Fe₃O₄@rGO/PANI, respectively (Details are available in section 2 of supplementary materials).

To characterize the morphology and microstructure of the ternary MGP NPs, TEM images are conducted and the results are presented in Fig. 1D. It is evident that

large-scale Fe_3O_4 nanoparticles with a relatively uniform size and granular structure are intercalated onto rGO sheets functionalized by PANI via a simple coprecipitation route. Besides, even if sonication was used during the preparation of TEM samples, these Fe_3O_4 nanoparticles are still firmly attached onto the sheets, which indicates there is an excellent adhesion between PANI-functionalized rGO sheets and Fe_3O_4 nanoparticles. The SAED pattern (inset in Fig. 1D) exhibited considerably sharp ring-like feature, revealing the polycrystalline feature of Fe_3O_4 .

Fig. 1 here

3.2 Electrochemical behavior of the sensors

EIS and CV were effective tools for probing the electrochemical properties of the sensor using $\text{Fe}(\text{CN})_6^{3-/4-}$ as probe and detailed electrochemical detection conditions were provided in supplementary materials. Fig. 2A illustrates the CV curves of the fabrication process. A couple of reversible redox peaks were obtained in curve a of bare MGCE. After modifying MGP NPs (curve b), an enhancement of peak currents of the electrode was observed, possibly owing to the large surface coverage and good electrochemical properties of MGP NPs. Before the elution of insulin from the EMMIPs, the peak current dropped obviously and the peak gap of the redox potential became wider (curve c) due to the electronically inert character of insulin. The peak value obviously increased after removing templates (curve d), indicating that imprinted cavities caused by the removal of insulin formed the channels for the probe $\text{Fe}(\text{CN})_6^{3-/4-}$ to reach the surface of the electrode. When the resultant EMMIPs reacted with excess insulin targets (curve e), the electron transfer of $\text{Fe}(\text{CN})_6^{3-/4-}$ was blocked

and the peak currents almost restored to the original value (before elution).

To investigate the electron transfer occurring at the electrodes, EIS measurements are also performed (Fig. 2B). The semicircle diameter equals the charge transfer resistance (R_{ct}) which represents the electron-transfer kinetics of the redox probe at the electrode interface.[42] The equivalent circuit model (inset of Fig. 2B) is used to fit the Nyquist plots, and the fitting parameters are listed in Table S1. The Nyquist plots for bare MGCE showed a small well-defined semicircle (curve a), indicating small interface impedance. Due to the large surface coverage and the good electronic transfer ability, the MGP NPs-modified MGCE (curve b) presented lower diameter ($R_{ct} = 226 \Omega$) than bare MGCE ($R_{ct} = 379 \Omega$). The assembly of EMMIPs onto the electrode increased the R_{ct} to 859Ω (curve c). After the elution of template (curve d), an obvious reduction of the semicircle diameter ($R_{ct} = 172 \Omega$) was observed. This R_{ct} was lower than that of MGP NPs-modified MGCE (curve b), indicated that the conductive imprinting layer over the ternary MGP NPs was successfully fabricated. When insulin was adsorbed to the imprinted cavities, the diameter ($R_{ct} = 788 \Omega$) almost resumed to the level before elution (curve e). These results are in agreement with those of CV method, validating that the prepared EMMIPs-based sensor could be preliminarily applied for the monitoring of insulin.

Fig. 2 here

3.3 Optimization of EMMIPs preparation conditions

Aniline acted as the co-monomer to interact with insulin as well as the cross-linker for forming imprinted membrane in the situ polymerization method. The

suitable ratio of insulin and aniline directly influenced the imprinting efficiency. As shown in Fig. 3A, the current response reached maximum when the concentration ratio of insulin to aniline was 1: 50. Low amount of aniline resulted in lacking of enough binding sites and poor electrochemical performance. However, superabundant aniline would lead to excessive cross-linking degree, making it difficult to remove templates. And too much aniline might pose difficulty in magnetic separation.

In pre-assembling process, MGP NPs interacted with template molecules through hydrogen bonding, hydrophobic action and π - π stacking interaction. Therefore, when the amount of MGP NPs was fixed, the optimization of the concentration of insulin was an important factor for studying the electrochemical properties of EMMIPs. When the concentration of template was higher than 0.4 g L^{-1} , templates tended to cluster, causing an augment in the size of imprinting cavities and thereby affecting the specificity and sensitivity of the EMMIPs. When the concentration of the target molecules was lower than 0.4 g L^{-1} , the DPV current was also reduced since a few number of cavities were fabricated. The EMMIPs had a highest current response with 0.4 g L^{-1} concentration of insulin (Fig. 3B).

The polymerization time during the synthetic process could control the thickness of PANI layer, which was closely related to imprinting effect. The prepared EMMIPs were conductive dark green product. When polymerization time was shorter than 4 h, the oxidation peak current of insulin in EMMIPs was poor. As extending the polymerization time, the I_p value of insulin increased, indicating the augment of the amount of insulin in EMMIPs. When polymerization time was more than 4 h, I_p value

reduced, demonstrating that insulin was embedded too deep to be eluted. Fig. 3C showed the optimal polymerization time was 4 h.

Fig. 3 here

3.4 Measurement of surface area

Methylene blue (MB) adsorption method was applied to measure the surface areas of EMMIPs and traditional MIES (fabricated by electro-polymerization).[43] Accordingly, 10 mg of EMMIPs and similarly prepared MIES were placed in 5 mL of MB solution of aware concentration for 12 h, respectively. A standard curve between absorbance at 618 nm and concentration of MB (32.5-325 $\mu\text{mol L}^{-1}$) was employed. From the MB concentration difference before and after adsorption onto the polymer, the amount of adsorbed MB could be predicted. The surface area was calculated by the following equation:

$$A_s = \frac{GN_{av}\Phi 10^{-20}}{MM_w}$$

where A_s is the surface area ($\text{m}^2 \text{g}^{-1}$), G is the amount of MB adsorbed (g), N_{av} is the Avogadro's number, Φ is the MB molecular cross-section (197.2 \AA^2), M_w is the molecular weight of MB (373.9 g mol^{-1}) and M is the mass of adsorbent (g).[43] EMMIPs presented higher surface area ($123.46 \text{ m}^2 \text{ g}^{-1}$) than traditional MIES fabricated by electro-polymerization ($49.36 \text{ m}^2 \text{ g}^{-1}$), indicating of more effective imprinting sites in the sensor fabricated by the magnetically controlled modification than the traditional electro-polymerization.

3.5 Control of the membrane

3.5.1 Advantages of magnetic field directed self-assembly

Our proposed EMMIPs-based sensor was fabricated by magnetic field directed self-assembly, and surface morphology of the sensor was uniform and dense characterized by SEM (Fig. S2). This indicated that magnetic field has been emerged as the driving force to direct the assembly of the EMMIPs, allowing nanostructures to be grown in a specific directional manner. Also, the immobilization and removal of EMMIPs on the electrode surface could be controlled freely by using an external magnet (Fig. S1).

3.5.2 Factors affecting the fabrication of the sensor

DPV method was used to explore the current of the sensor prepared with various magnetic field strengths and EMMIPs concentrations, respectively. As shown in the histogram of Fig. 4, the highest current response was achieved by the sensor fabricated with the modest magnetic field strength and EMMIPs concentration. And each magnetic field strength of the MGCE had the most suitable concentration of EMMIPs to fabricate the sensor with highest current. When the concentration of EMMIPs was constant, the amount of the EMMIPs absorbed to the surface of the electrode rose with the increasing magnetic field strength, leading to the growth of the current response of the sensor. However, high magnetic field strength probably caused the over-rapid aggregation of the EMMIPs and low current response was obtained. These results indicated that the fabrication of the membrane depends on the interaction between the EMMIPs and magnetic field, and a desired membrane with high sensitivity can be achieved based on moderate interaction. Adjusting the magnetic field strength and altering EMMIPs concentrations were observed to be two

strategies to control the sensor.

3.5.3 AFM Characterization of the sensor prepared with various magnetic fields

The morphology of the MIPs membranes fabricated with various magnetic fields was further investigated by AFM, and the images were obtained using tapping mode. As shown in Fig. 4A-F, the sensor surface exhibits an island-like structure and the surface islands of the sensor prepared with magnetic field appear in clusters and well-distributed. The roughness of D-F was about 21.1 nm, 35.9 nm, and 81.2 nm, respectively, and the cluster became larger with the increase of the magnetic field strength. This indicated that the nanostructure of membrane could be easily controlled at the microscopic level by varying the magnetic field strength of MGCE.

Fig. 4 here

3.6 Evaluation of the adsorption characteristics

The adsorption isotherms of EMMIPs and EMNIPs to insulin were plotted in Fig. 5A. As the concentration of the templates increased, the current of EMMIPs-based sensor rose quickly until equilibrium, while the current of EMNIPs-based sensor remained almost constant. It exhibited the EMMIPs had a better performance of memory function and adsorption ability for insulin.

The adsorption and desorption kinetics of EMMIPs was investigated with 25 nM insulin solution at different time points. As Fig. 5B showed, EMMIPs reached adsorption and desorption equilibrium within approximately 20 min and 15 min, respectively, indicating that EMMIPs has excellent kinetics performance.

Fig. 5 here

3.7 Molecular recognition

To investigate the selectivity of EMMIPs-based sensor, we actualized the competitive recognition under the optimum conditions in a mixture of three proteins (BSA, BHB and HRP) with equal concentration and four possible coexisting small molecules (UA 200 $\mu\text{mol L}^{-1}$, AA 100 $\mu\text{mol L}^{-1}$, DA 0.25 $\mu\text{mol L}^{-1}$ and 0.25 $\mu\text{mol L}^{-1}$ GSH, considering their normal physiological levels) over 2.5 nmol L^{-1} insulin, respectively. The anti-interference property of the sensor was evaluated via calculating the DPV current assayed in the presence and absence of interference components, respectively. Fig. 5C revealed that the presence of small molecules can hardly cause the obvious change of the response current of insulin (current% varied from 94% to 104%) while the presence of macromolecules had a mild effect on the current ratio (current% varied from 87% to 90%). Moreover, the effect of some ions (Na^+ , K^+ , Mg^{2+} , Ca^{2+} , Cl^- , HCO_3^-) co-coexisting with insulin was investigated as their concentrations were 100 times higher than that of insulin. In Fig. S6, these ions did not interfere with the detection. These results demonstrated that the imprinted sensor can avoid the interference of the coexisting components and ions that existed commonly in biological samples and thus can allow the detection of insulin in a complex matrix. The selectivity performance of the sensor might be attributed to the multiple recognition sites in the EMMIPs for specifically recognizing target molecules. Therefore, the imprinted sensor can be used as recognition material to the selective determination of insulin.

3.8 Reproducibility and stability

To explore the reproducibility of the EMMIPs-based sensor, the experiments were performed in 2.5 nM insulin. The proposed sensor was regenerated with a peak current RSD of 4.8% using three different EMMIPs obtained from three separate synthesis reactions. The excellent reuse capacity was obtained with a RSD of 6.3% calculated using EMMIPs with 10 times of elution, adsorption and measurement. The stability of the sensor is also an important factor to be considered. The EMMIP was stored for about 20 days, and current response of insulin retained at 90% compared to recently synthesized EMMIP, indicating excellent stability.

3.9 Calibration curve and detection limit

The DPV responses of EMMIPs adsorbing insulin with different concentrations were further evaluated under optimal working conditions. Related oxidation mechanism were discussed in section 6 of supplementary materials. The DPV currents suggest an oxidation of electroactive tyrosine residues in the insulin molecule. Two calibration curves between the peak currents and different insulin concentrations were obtained and the limit of detection of this method was 17 pM (S/N = 3). The details were specified in section 7 of supplementary materials.

By diagnosing the levels of insulin, one can predict the type of diabetic. However, the level of insulin in blood serum was on the order of picomolar. We therefore used the soluble $\text{Fe}(\text{CN})_6^{3-/4-}$ redox probe to further improve the sensitivity of the proposed method. Similar to the operation described in section 2.5, the EMMIPs were magnetically absorbed to the surface of MGCE after the binding with different concentrations of insulin, and then DPV method was conducted in PB

solution (0.02 M, pH 7.4) containing 10 mM $\text{Fe}(\text{CN})_6^{3-/4-}$ and 0.1 M KCl. As expected, the DPV current signals of the $\text{Fe}(\text{CN})_6^{3-/4-}$ probe decreased with the binding of increasing insulin concentration-EMMIPs adsorbed to the MGCE (Fig. 6A). A calibration curve between the concentration of insulin and the peak current was obtained (Inset of Fig. 6A) and could be described as $I_p (\mu\text{A}) = -16.09C (\text{nM}) + 87.27$ ($R^2 = 0.978$) in the range of 0.01-1 nM, with a detection limit of 3 pM. It is likely that this sensitivity is, at least partially, aided by the insulin negative charge (the isoelectric point of human insulin is about 5.4[44]) at pH 7.4 and the resulting electrostatic repulsion of the negatively charged redox probe. The comparison of our sensor with other reported sensors in determining insulin is summarized in section 8 of the supplementary materials.

Fig. 6 here

3.10 Application to real serum samples

Our ultimate goal is to employ the proposed method for the diagnosis and classification of diabetes. Therefore, the insulin levels of 18 serum samples from diabetic patients and healthy volunteers under a fasting condition were quantified by the EMMIPs based sensor (Fig. 6B). The normal level of serum insulin under a fasting condition is 5-25 mIU L⁻¹ (35-173 pM), whereas lower or higher concentrations are characteristic of type 1 and onset of type 2 diabetes, respectively.[45-46] From the red dots in Fig. 6B, 3 patients (insulin levels: 28.93-31.30 pM) were diagnosed with type 1 diabetic while 6 patients (insulin levels: 183.54-223.39 pM) suffered from type 2 diabetic. And the insulin levels of the others

(48.71-120.61 pM) were within the normal range. The analysis results were further compared to those obtained by radioimmunoassay used clinically (black dots of Fig. 6B). For statistical analysis, a paired t-test and linear regression analysis between the two methods was performed. The t value 0.645 were less than t_{crit} ($t_{crit[17, 0.05]} = 2.110$). Moreover, the linear regression equation was $y = 0.9991x - 0.0258$ ($R^2 = 0.989$, x-axis: by our method; y-axis: by radioimmunoassay). The slope and intercept of the equation were near to the ideal values 1 and 0, respectively. These results indicated a good consistency between both methods. Furthermore, as shown in Table S4, our proposed EMMIPs based sensor shows several advantages in rapid, simple and convenient detection, easy operation, low cost and low pollution compared with the clinically available radioimmunoassay. These results suggested that our proposed EMMIPs-based sensor showed potential value for clinical determination of insulin.

4. Conclusions

A facile and controllable EMMIPs-based sensor was fabricated via magnetic field directed self-assembly for the measurement of insulin in real biological samples. The multifunctional EMMIPs with large surface area, excellent conductivity, magnetic response and selectivity recognition properties were obtained on the surface of ternary MGP NPs under mild condition. The EMMIPs-based sensor showed good sensitivity, selectivity, and efficiency for insulin detection in biological samples.

We summarized the superior merits of the as-obtained sensor as follows: (i) By magnetic field directed self-assembly, the EMMIPs could be fast oriented and assembled orderly on the surface of the electrode to form sensitive electrochemical

sensor; (ii) The membrane could be easily fabricated or removed by using a freely controllable external magnet, and also, it could be controlled by adjusting the magnetic field strength or altering EMMIPs concentrations; (iii) The regeneration of the electrode after use is simple and efficient; (iv) All steps of this method were completed independently, so the efficiency of the analysis was improved. We believe that this sensor is an improved detection method for biomarkers, and a valuable tool with potential applications in high throughput analysis for clinical diagnosis.

Acknowledgments

This work was supported by National Natural Science Foundation of China (Nos. 81572081, 81273480, 21175070), Natural Science Foundation of Jiangsu Province (No.BK20141433) and Graduate Innovation Project of Jiangsu Province (No.KYZZ16_399).

References:

- [1] E. Martínez-Peri Án, M. Revenga-Parra, M. Gennari, F. Pariente, R. Mas-Ballesté, F. Zamora and E. Lorenzo, Insulin sensor based on nanoparticle-decorated multiwalled carbon nanotubes modified electrodes, *Sens. Actuators, B* 222 (2016) 331-338.
- [2] V. Singh and S. Krishnan, Voltammetric immunosensor assembled on carbon-pyrenyl nanostructures for clinical diagnosis of type of diabetes, *Anal. Chem.* 87 (2015) 2648-2654.
- [3] M. Xu, X. Luo and J.J. Davis, The label free picomolar detection of insulin in blood serum, *Biosens. Bioelectron.* 39 (2013) 21-25.
- [4] J.R. Lindsay, A.M. McKillop, M.H. Mooney, F.P. O'Harte, P.M. Bell and P.R. Flatt, Demonstration of increased concentrations of circulating glycosylated insulin in human Type 2 diabetes using a novel and specific radioimmunoassay, *Diabetologia* 46 (2003) 475-478.
- [5] Y. Wang, D. Gao, P. Zhang, P. Gong, C. Chen, G. Gao and L. Cai, A near infrared fluorescence resonance energy transfer based aptamer biosensor for insulin detection in human plasma, *Chem. Commun.* 50 (2014) 811-813.
- [6] M.S. Even, C.B. Sandusky, N.D. Barnard, J. Mistry and M.K. Sinha, Development of a novel ELISA for human insulin using monoclonal antibodies produced in serum-free cell culture medium, *Clin. Biochem.* 40 (2007) 98-103.
- [7] X. Zhang, S. Zhu, C. Deng and X. Zhang, An aptamer based on-plate microarray for high-throughput insulin detection by MALDI-TOF MS, *Chem. Commun.* 48 (2012) 2689-2691.
- [8] Y. Yu, M. Guo, M. Yuan, W. Liu and J. Hu, Nickel nanoparticle-modified electrode for ultra-sensitive electrochemical detection of insulin, *Biosens. Bioelectron.*

77 (2016) 215-219.

[9] J.Y. Gerasimov, C.S. Schaefer, W. Yang, R.L. Grout and R.Y. Lai, Development of an electrochemical insulin sensor based on the insulin-linked polymorphic region, *Biosens. Bioelectron.* 42 (2013) 62-68.

[10] M. Jaafariasl, E. Shams and M.K. Amini, Silica gel modified carbon paste electrode for electrochemical detection of insulin, *Electrochim. Acta* 56 (2011) 4390-4395.

[11] W. Zhu, G. Jiang, L. Xu, B. Li, Q. Cai, H. Jiang and X. Zhou, Facile and controllable one-step fabrication of molecularly imprinted polymer membrane by magnetic field directed self-assembly for electrochemical sensing of glutathione, *Anal. Chim. Acta* 886 (2015) 37-47.

[12] T. Wen, W. Zhu, C. Xue, J. Wu, Q. Han, X. Wang, X. Zhou and H. Jiang, Novel electrochemical sensing platform based on magnetic field-induced self-assembly of Fe₃O₄@Polyaniline nanoparticles for clinical detection of creatinine, *Biosens. Bioelectron.* 56 (2014) 180-185.

[13] J. Kupis-Rozmys Owicz, M. Wagner, J. Bobacka, A. Lewenstam and J. Migdalski, Biomimetic membranes based on molecularly imprinted conducting polymers as a sensing element for determination of taurine, *Electrochim. Acta* 188 (2016) 537-544.

[14] V.K. Gupta, M.L. Yola, N. Zalt N, N. Atar, Z. Üstünda and L. Uzun, Molecular imprinted polypyrrole modified glassy carbon electrode for the determination of tobramycin, *Electrochim. Acta* 112 (2013) 37-43.

[15] Q. Li, K. Yang, Y. Liang, B. Jiang, J. Liu, L. Zhang, Z. Liang and Y. Zhang, Surface protein imprinted core-shell particles for high selective lysozyme recognition prepared by reversible addition-fragmentation chain transfer strategy, *ACS Appl.*

Mater. Inter. 6 (2014) 21954-21960.

[16] L. Liu, T. Zhong, Q. Xu and Y. Chen, Efficient Molecular Imprinting Strategy for Quantitative Targeted Proteomics of Human Transferrin Receptor in Depleted Human Serum, *Anal. Chem.* 87 (2015) 10910-10919.

[17] X. Bi and Z. Liu, Facile preparation of glycoprotein-imprinted 96-well microplates for enzyme-linked immunosorbent assay by boronate affinity-based oriented surface imprinting, *Anal. Chem.* 86 (2014) 959-966.

[18] L. Qian, X. Hu, P. Guan, D. Wang, J. Li, C. Du, R. Song, C. Wang and W. Song, The effectively specific recognition of bovine serum albumin imprinted silica nanoparticles by utilizing a macromolecularly functional monomer to stabilize and imprint template, *Anal. Chim. Acta* 884 (2015) 97-105.

[19] G. Guan, Z. Zhang, Z. Wang, B. Liu, D. Gao and C. Xie, Single-Hole Hollow Polymer Microspheres toward Specific High-Capacity Uptake of Target Species, *Adv. Mater.* 19 (2007) 2370-2374.

[20] D. Gao, Z. Zhang, M. Wu, C. Xie, G. Guan and D. Wang, A surface functional monomer-directing strategy for highly dense imprinting of TNT at surface of silica nanoparticles, *J. Am. Chem. Soc.* 129 (2007) 7859-7866.

[21] R. Gao, Y. Hao, L. Zhang, X. Cui, D. Liu, M. Zhang, Y. Tang and Y. Zheng, A facile method for protein imprinting on directly carboxyl-functionalized magnetic nanoparticles using non-covalent template immobilization strategy, *Chem. Eng. J.* 284 (2016) 139-148.

[22] J. Guo, Y. Wang, Y. Liu, C. Zhang and Y. Zhou, Magnetic-graphene based molecularly imprinted polymer nanocomposite for the recognition of bovine hemoglobin, *Talanta* 144 (2015) 411-419.

[23] R. Gao, L. Zhang, Y. Hao, X. Cui, D. Liu, M. Zhang and Y. Tang, Novel

- polydopamine imprinting layers coated magnetic carbon nanotubes for specific separation of lysozyme from egg white, *Talanta* 144 (2015) 1125-1132.
- [24] Y. Lv, T. Tan and F. Svec, Molecular imprinting of proteins in polymers attached to the surface of nanomaterials for selective recognition of biomacromolecules, *Biotechnol. Adv.* 8 31 (2013) 1172-1186.
- [25] Z. Ding, S.W. Annie Bligh, L. Tao, J. Quan, H. Nie, L. Zhu and X. Gong, Molecularly imprinted polymer based on MWCNT-QDs as fluorescent biomimetic sensor for specific recognition of target protein, *Mat. Sci. Eng, C* 48 (2015) 469-479.
- [26] R. Ouyang, J. Lei and H. Ju, Artificial receptor-functionalized nanoshell: facile preparation, fast separation and specific protein recognition, *Nanotechnology* 21 (2010) 185502.
- [27] Z. Xia, Z. Lin, Y. Xiao, L. Wang, J. Zheng, H. Yang and G. Chen, Facile synthesis of polydopamine-coated molecularly imprinted silica nanoparticles for protein recognition and separation, *Biosens. Bioelectron.* 47 (2013) 120-126.
- [28] Y. Li, Y. Liu, Y. Yang, F. Yu, J. Liu, H. Song, J. Liu, H. Tang, B.C. Ye and Z. Sun, Novel electrochemical sensing platform based on a molecularly imprinted polymer decorated 3D nanoporous nickel skeleton for ultrasensitive and selective determination of metronidazole, *ACS Appl. Mater. Inter.* 7 (2015) 15474-15480.
- [29] C. Xue, X. Wang, W. Zhu, Q. Han, C. Zhu, J. Hong, X. Zhou and H. Jiang, Electrochemical serotonin sensing interface based on double-layered membrane of reduced graphene oxide/polyaniline nanocomposites and molecularly imprinted polymers embedded with gold nanoparticles, *Sens. Actuators, B* 196 (2014) 57-63.
- [30] C. Zhang, W. Bai and Z. Yang, A novel photoelectrochemical sensor for bilirubin based on porous transparent TiO₂ and molecularly imprinted polypyrrole, *Electrochim. Acta* 187 (2016) 451-456.

- [31] X. Wang, X. Li, C. Luo, M. Sun, L. Li and H. Duan, Ultrasensitive molecularly imprinted electrochemical sensor based on magnetism graphene oxide/ β -cyclodextrin/Au nanoparticles composites for chrysoidine analysis, *Electrochim. Acta* 130 (2014) 519-525.
- [32] B. Rezaei, M.K. Boroujeni and A.A. Ensafi, A novel electrochemical nanocomposite imprinted sensor for the determination of lorazepam based on modified polypyrrole@sol-gel@gold nanoparticles/pencil graphite electrode, *Electrochim. Acta* 123 (2014) 332-339.
- [33] Y. Pan, L. Shang, F. Zhao and B. Zeng, A novel electrochemical 4-nonyl-phenol sensor based on molecularly imprinted poly (o-phenylenediamine-co-o-toluidine) -nitrogen-doped graphene nanoribbons-ionic liquid composite film, *Electrochim. Acta* 151 (2015) 423-428.
- [34] M. Duan, R. Liang, N. Tian, Y. Li and E.S. Yeung, Self-assembly of Au-Pt core-shell nanoparticles for effective enhancement of methanol electrooxidation, *Electrochim. Acta* 87 (2013) 432-437.
- [35] B. Dong, T. Zhou, H. Zhang and C.Y. Li, Directed self-assembly of nanoparticles for nanomotors, *ACS Nano* 7 (2013) 5192-5198.
- [36] H. Zhang, B. Dong, T. Zhou and C.Y. Li, Directed self-assembly of hetero-nanoparticles using a polymer single crystal template, *Nanoscale* 4 (2012) 7641-7645.
- [37] Q. Han, X. Wang, Z. Yang, W. Zhu, X. Zhou and H. Jiang, Fe(3)O(4)@rGO doped molecularly imprinted polymer membrane based on magnetic field directed self-assembly for the determination of amaranth, *Talanta* 123 (2014) 101-108.
- [38] T. Wen, W. Zhu, C. Xue, J. Wu, Q. Han, X. Wang, X. Zhou and H. Jiang, Novel electrochemical sensing platform based on magnetic field-induced self-assembly of

- Fe₃O₄@Polyaniline nanoparticles for clinical detection of creatinine, *Biosens. Bioelectron.* 56 (2014) 180-185.
- [39] P. Liu, Y. Huang and X. Zhang, Synthesis and excellent microwave absorption properties of graphene/polypyrrole composites with Fe₃O₄ particles prepared via a co-precipitation method, *Mater. Lett.* 129 (2014) 35-38.
- [40] P. Xiong, C. Hu, Y. Fan, W. Zhang, J. Zhu and X. Wang, Ternary manganese ferrite/graphene/polyaniline nanostructure with enhanced electrochemical capacitance performance, *J. Power Sources* 266 (2014) 384-392.
- [41] L. Wang, Y. Huang, C. Li, J. Chen and X. Sun, Hierarchical composites of polyaniline nanorod arrays covalently-grafted on the surfaces of graphene@Fe₃O₄@C with high microwave absorption performance, *Compos. Sci. Technol.* 108 (2015) 1-8.
- [42] J. Li, P. Wu, F. Lou, P. Zhang, Y. Tang, Y. Zhou and T. Lu, Mesoporous carbon anchored with SnS₂ nanosheets as an advanced anode for lithium-ion batteries, *Electrochim. Acta* 111 (2013) 862-868.
- [43] B.B. Prasad, R. Madhuri, M.P. Tiwari and P.S. Sharma, Imprinting molecular recognition sites on multiwalled carbon nanotubes surface for electrochemical detection of insulin in real samples, *Electrochim. Acta* 55 (2010) 9146-9156.
- [44] M. Xu, X. Luo and J.J. Davis, The label free picomolar detection of insulin in blood serum, *Biosens. Bioelectron.* 39 (2013) 21-25.
- [45] A.K. Yagati, Y. Choi, J. Park, J. Choi, H. Jun and S. Cho, Silver nanoflower–reduced graphene oxide composite based micro-disk electrode for insulin detection in serum, *Biosens. Bioelectron.* 80 (2016) 307-314.
- [46] C. Weyer, R.L. Hanson, P.A. Tataranni, C. Bogardus and R.E. Pratley, A high fasting plasma insulin concentration predicts type 2 diabetes independent of insulin resistance: evidence for a pathogenic role of relative hyperinsulinemia, *Diabetes* 12 49

(2000) 2094-2101.

Figure captions:

Fig. 1 XPS spectra of survey scan (A), Fe 2p (inset in A), C 1s (B) and N 1s (C) for MGP NPs. (D) TEM images of ternary MGP NPs (Inset: the SAED pattern of MGP NPs).

Fig. 2 (A) Cyclic voltammograms of 10 mM $\text{Fe}(\text{CN})_6^{3-/4-}$ and 0.1 M KCl at bare MGCE (a), MGCE modified with MGP NPs (b), EMMIPs-based sensor before (c) and after elution (d), EMMIPs-based sensor adsorption of insulin(e). (B) Nyquist plots for EIS measurements of 10 mM $\text{Fe}(\text{CN})_6^{3-/4-}$ and 0.1 M KCl at bare MGCE (a), MGCE modified with MGP NPs (b), EMMIPs-based sensor before (c) and after elution (d), EMMIPs-based sensor adsorption of insulin(e). The inset of B is the equivalent circuit for the EIS test.

Fig. 3 The optimal results of EMMIPs preparation. (A) the molar ratio of insulin to aniline ($C_{\text{insulin}} : C_{\text{aniline}}$), (B) the concentration of insulin (C_{insulin}), (C) incubation time.

Fig. 4 (Histogram) DPV current response of the EMMIPs-based sensor prepared with various magnetic field strengths of the MGCE and different EMMIPs concentration, respectively. AFM images (A-C) and 3D AFM images (D-F) of the sensor prepared with 0.032 T, 0.128 T and 0.256 T magnetic field strength of MGCE, respectively.

Fig. 5 (A) The adsorption isotherms of EMMIPs and ENNIPs. (B) Adsorption and desorption kinetics of EMMIPs. (C) DPV Peak current of the EMMIPs-based sensor to 2.5 nmol L^{-1} insulin in the presence of BSA, BHB, HRP, UA, DA, AA or GSH, respectively.

Fig. 6 (A) DPV current signals of the $\text{Fe}(\text{CN})_6^{3-/4-}$ probe of EMMIPs adsorbed to the MGCE after the binding of insulin with increasing concentration (a-h: 0.01-1 nM); the inset: the calibration curve. (B) The assay results of insulin levels for human serum samples by using our method (red dots) and the radioimmunoassay (black dots).

Scheme 1 Schematic representation for the preparation of EMMIPs and the process of electrochemical detection.

Fig. 1

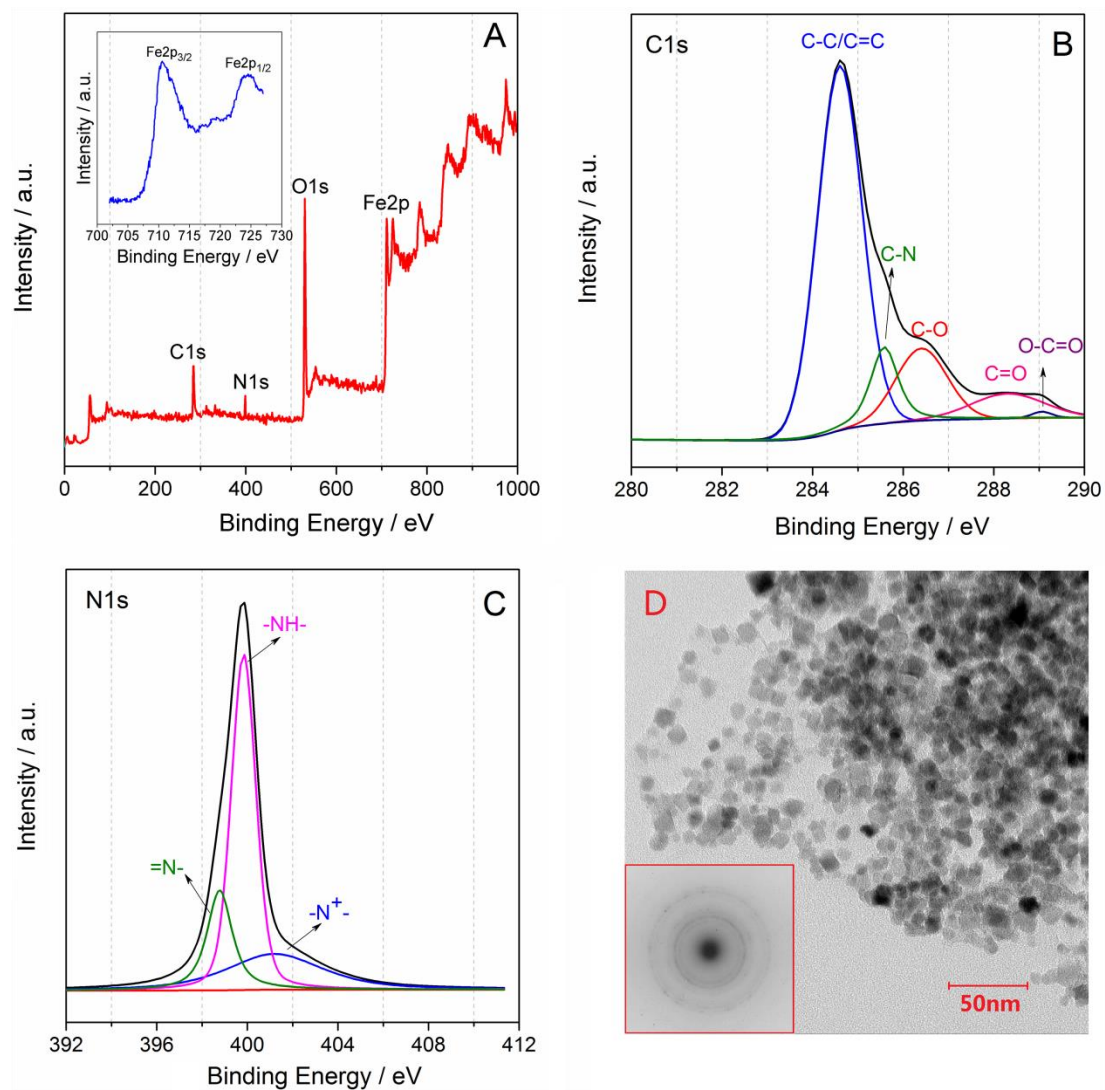


Fig. 2

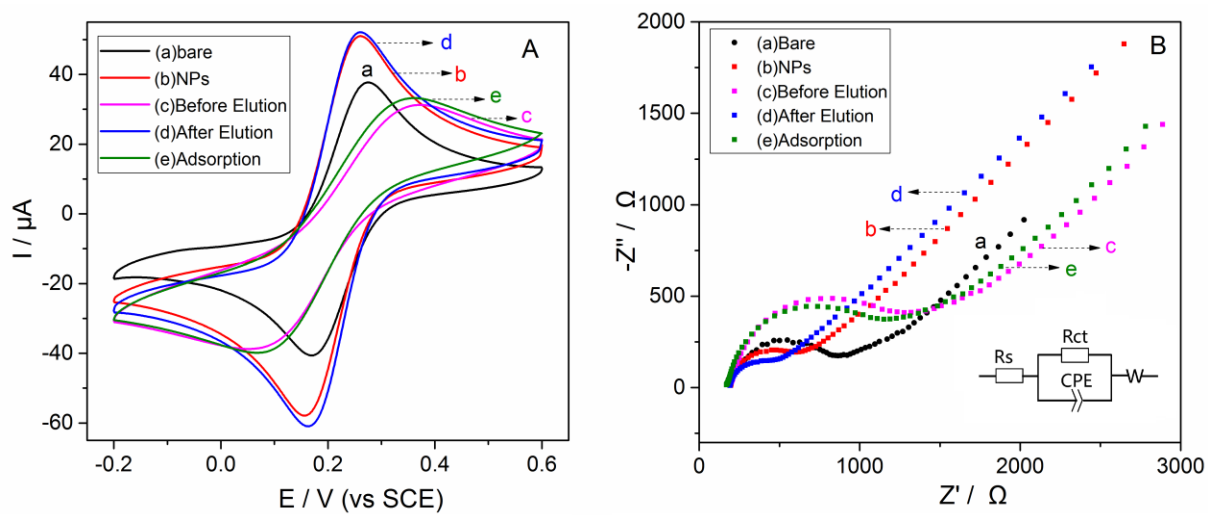


Fig. 3

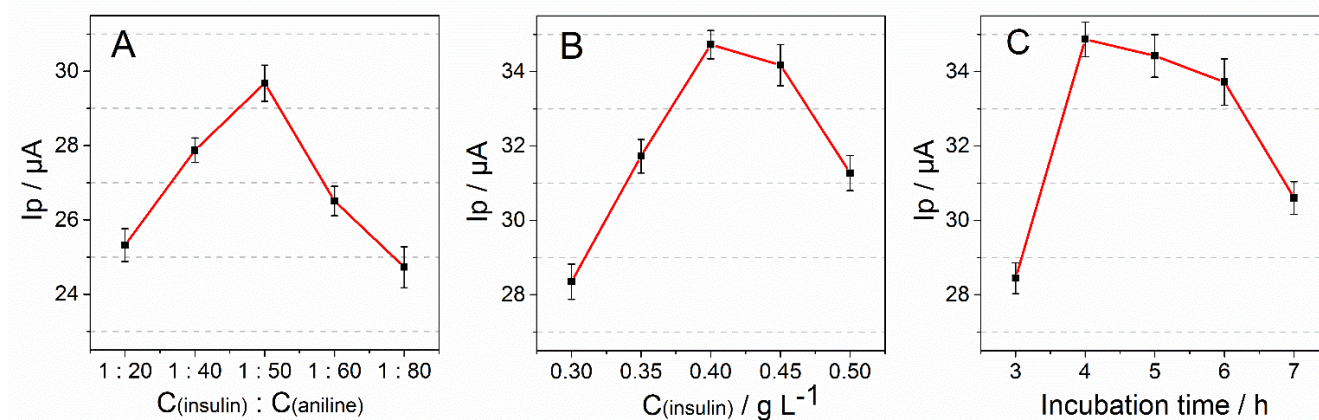


Fig. 4

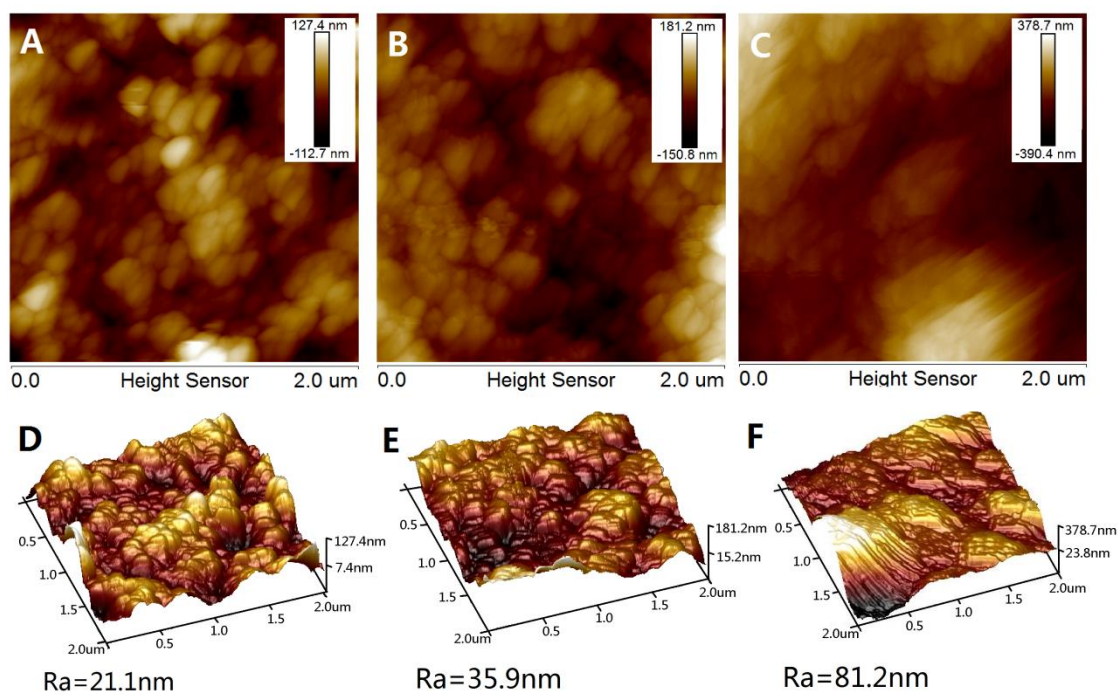
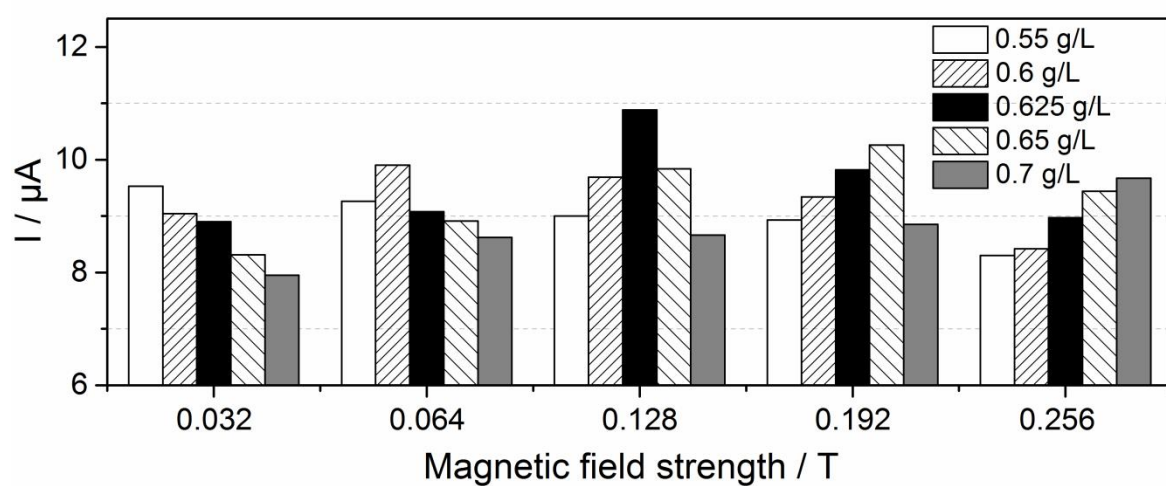


Fig. 5

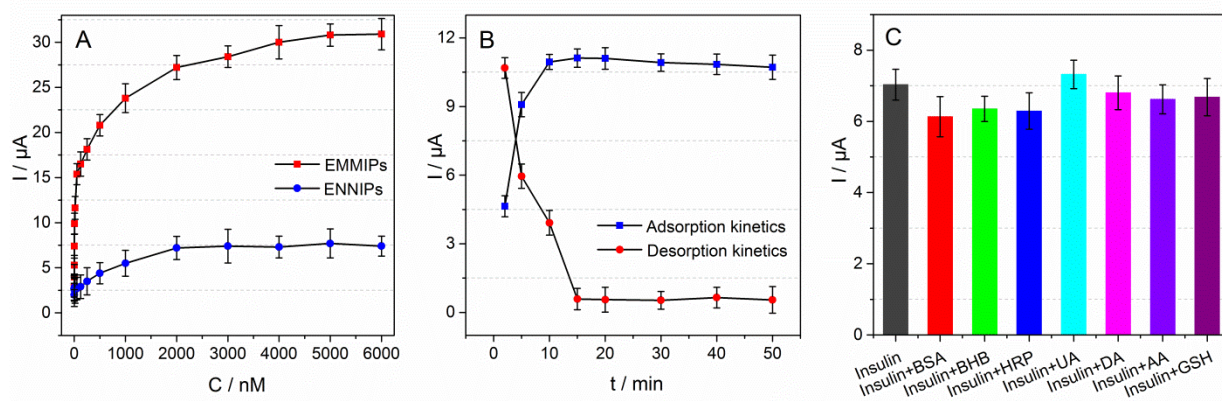
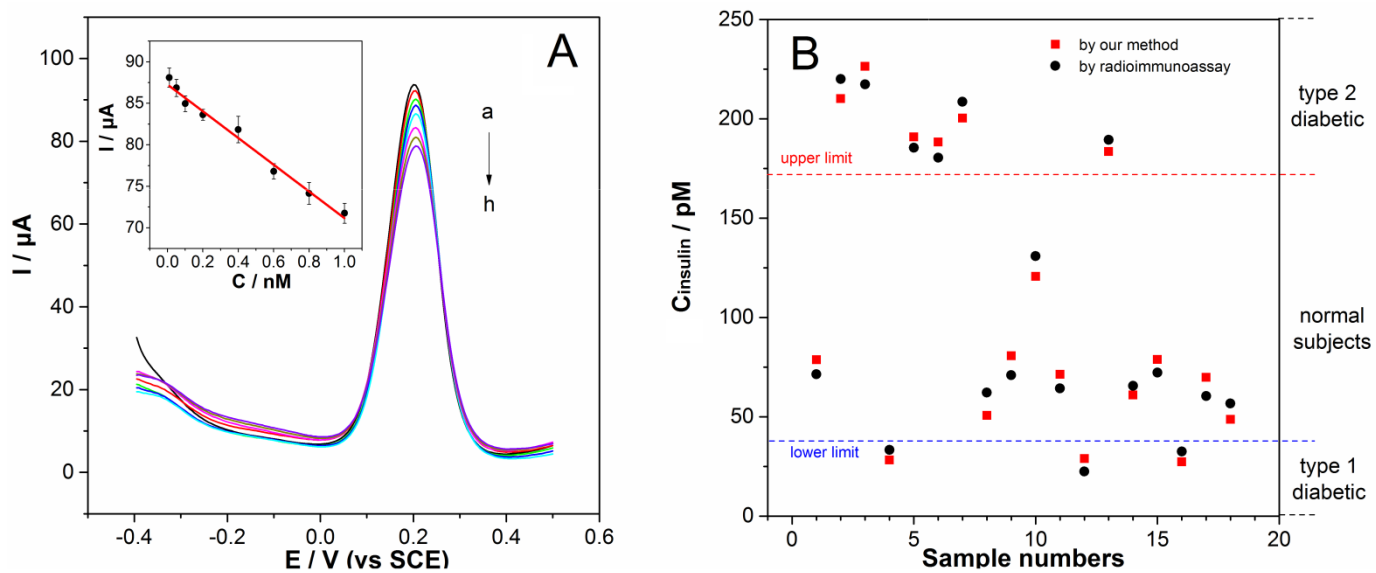


Fig.6



Scheme 1

